11th International Conference on Green Energy & Environmental Engineering (GEEE-2025)
Proceedings of Engineering & Technology – PET-Vol 94, pp.33-38

Non-Destructive Electro-Pyroelectric Characterization of Cr-Doped GaAs: A Thermal–Electrical Crucial Tool for Advanced Semiconductor Engineering

Imen Mellouki[*1], Nawel Khaldi[1], Sofiene Ilahi[2] and Mariem Lazaar[1]

[1]*Thermal Process Laboratory, Research and Technology Center of Energy, Borj-Cedria Science and Technology Park, Nabeul, Tunisia.*
[2]*Photo-Thermal Characterization Research Laboratory, Preparatory Institute for Engineering Studies of Nabeul, B. P. 62, 8000, Nabeul, Tunisia.*
[*]imene.mellouki@ipeit.rnu.tn

Abstract—We present the non‐destructive electro-pyroelectric (EPE) technique for simultaneously measuring thermal parameters and electrical AC resistivity in bulk semiconductors at room temperature. Conventional characterization methods often suffer from laser-induced heating artifacts and complex calibration procedures, which limit their accuracy and efficiency. In response, our approach utilizes a 25 µm PVDF sensor combined with frequency-modulated Joule heating to generate thermal waves, employing two complementary configurations: Front EPE (FEPE) and Inverse EPE (IEPE). The FEPE mode enables precise direct measurements of thermal conductivity (κ) and diffusivity (D), while the IEPE configuration integrates broadband AC impedance spectroscopy to determine electrical resistivity (ρ). Validation on MBE-grown Cr-doped GaAs confirms that the measured parameters closely match theoretical predictions, thereby demonstrating that the EPE technique is both reliable and cost-effective. The findings strongly suggest that this methodology not only overcomes the limitations of conventional approaches but also holds significant promise for advancing semiconductor characterization in emerging high-frequency applications.

***Keywords*— Electro-pyroelectric, Cr-doped GaAs, semiconductor characterization, thermal conductivity, thermal diffusivity, electrical resistivity, non-destructive testing, frequency-modulated Joule heating**

I. INTRODUCTION

This work employs the non-destructive and cost-effective ElectroPyroElectric (EPE) Technique [1] to simultaneously measure thermal conductivity, thermal diffusivity, and electrical resistivity in semiconductor substrates. Traditional methods such as photopyroelectric (PPE) approaches [2] are hampered by laser-induced heating artifacts and complex infrared calibration, while techniques like lock-in thermography (LIT) [3] struggle with phonon scattering challenges inherent in Raman thermometry. In contrast, the EPE technique uses a 25 µm thick polyvinylidene fluoride (PVDF) pyroelectric detector pressed against the sample and heated via frequency-modulated Joule heating (ranging from 0.1 Hz to 50 kHz). A 125 µm Mylar film is interposed to avoid short-circuiting, ensuring that the measured temperature primarily reflects that of the sample. This paper details the theoretical basis, experimental implementation, and validation of the EPE method, illustrating its effectiveness as an alternative characterization tool for advanced semiconductor engineering.

The methodology is structured around two complementary configurations of the EPE technique. In the Front EPE (FEPE) configuration, the heating electrodes are in direct contact with the PVDF sensor. This arrangement is specifically optimized for obtaining direct measurements of thermal conductivity and diffusivity. Transitioning to the Inverse EPE (IEPE) setup, the sample itself serves as the heating transducer. Herein, the FEPE-derived thermal parameters are incorporated into a comprehensive AC impedance model that enables the extraction of electrical resistivity. In both configurations, the experimental conditions are

ISSN: 1737-9334

carefully controlled within a specified frequency range (FEPE: 0.1 Hz to 100 Hz; IEPE: 200 Hz to 50 kHz), ensuring consistency and reproducibility throughout the measurement process.

II. THEORETICAL MODEL OF EPE DETECTION

The electro-pyroelectric (EPE) configuration, schematically represented in Fig. 1, is made of five adjacent layers: air (a), sample (s), Mylar layer (g), PVDF film (p) and backing (b). Mylar layer was chosen to create close thermal contact between the sample and the PVDF sensor, ensuring that the temperature measured by the PVDF sensor reflects mainly the sample's temperature rather than external influences [4]. In the PyroElectric system, the propagation of thermal waves is intricately governed by the thermal diffusion length (μ), which is variable through a straightforward adjustment of the modulation frequency (f); μ denotes the penetration depth of the thermal wave through the PyroElectric (PE) cell layer. Given the uniform heating of the sample, our approach considers a one-dimensional (1-D) heat treatment, treating the spatial average Pyroelectric voltage $\langle V_p(\omega)\rangle$ as a function of frequency modulation f.

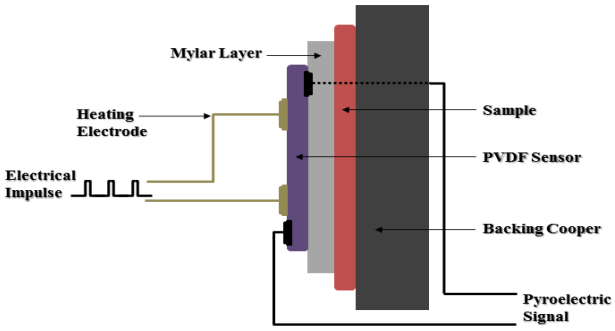

Fig. 1.a Schematic view of the Front detection configuration of PE cell.

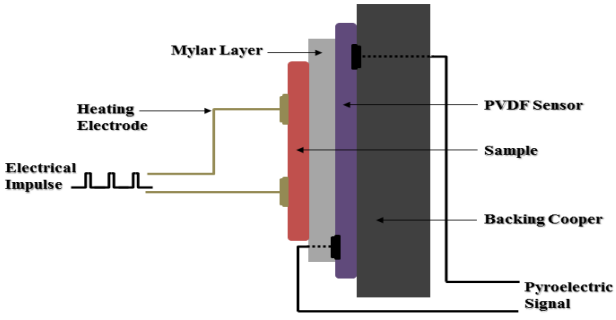

Fig. 1.b Schematic view of the Inverse detection configuration of PE cell.

The expression for the pyroelectric signal is derived by solving the heat equations across the various layers of the theoretical model, as detailed in our previous work [5]-[6]. Optimization of the parameter set concerning the PE cell design can be achieved by analyzing two specific detection configurations within the EPE technique. The first configuration, known as the Front EPE (FEPE), involves heating electrodes in direct contact with the sensor (Fig. 1.a). Accordingly, the second referred to as the Inverse EPE (IEPE), places the heating electrodes in direct contact with the sample (Fig. 1.b). To maintain the experimental conditions, we have imposed a frequency range from 100mHz to 100Hz. The spatial average pyroelectric voltage $\langle V_p^F(\omega)\rangle$ in Front detection is given by the following equation:

$$\langle V_p^F(\omega)\rangle = -\frac{1}{(jw\tau_e+1)(jw\tau_{th}+1)}\times\frac{A_v S\Lambda\phi(w)\tau_{th}\tau_e\tau I_e^2}{C_p C_{thp} C_{ths}} \times\left(\frac{\left([b_{bg}+\sigma_s l_s(b_{bs}+b_{sg})+1\right]e^{\sigma_g l_g}+\left[b_{bg}-\sigma_s l_s(b_{bs}-b_{sg})-1\right]e^{-\sigma_g l_g}\right)b_{gp}}{(b_{ga}+1)(b_{bg}+1)\,e^{\sigma_g l_g}+(b_{ga}+1)(b_{bg}-1)\,e^{-\sigma_g l_g}}+1\right)Z_p(w) \quad (1)$$

In equation (1), $\phi(w)$ represents the electrical heating power, I_e denotes the current intensity, τ_e stands for the detector's electrical time-constant, and τ_{th} refers to the detector's thermal time-constant. Additionally, the electrical pulse duration τ ($1\mu s$) is assumed to be sufficiently brief to neglect additional heat losses and satisfies the condition $\tau \ll \tau_e \ll \tau_{th}$. The coefficients Λ, A_v , S, C_{thp}, $C_p$and C_{ths} respectively represent the pyroelectric parameter of the PVDF sensor, the gain of the amplifier, the surface area of the sample, the specific heat capacity of the detector, the pyroelectric material capacitance, and the specific heat capacity of the sample. D_i and l_i represent the thermal diffusivity and thickness of medium i *(*where i = *a, s, g, p, b)*. The thermal diffusivity D_i correlated with the thermal conductivity K_i as follows: $D_i = \frac{K_i}{\rho_i c_i}$, where $\rho_i c_i$ is the specific heat volume. μ_i is the thermal diffusion length of medium i, defined by $\sigma_i = \frac{1+j}{\mu_i}$, and $\frac{1}{\mu_i} =$

ISSN: 1737-9334

$\left(\frac{\pi f}{D_i}\right)^{1/2}$, $b_{ij} = \frac{K_i \sigma_i}{K_j \sigma_j}$ is the thermal transport coefficient, and $Z_p(w)$ represents the electrical impedance of the PVDF sensor. It is revealed that the FEPE configuration, in this specific case, serves as a sensitive and reliable tool for concurrently assessing the thermal conductivity (K_s) and thermal diffusivity (D_s) of substrates. However, obtained thermal values from the analysis of the studied sample in FEPE case, are incorporated into the Inverse EPE detection method, applying the limit case for a thermally thick sample ($\mu_s \gg l_s$). Consequently, a frequency range was imposed from 200 Hz to approximately 50 kHz. The expression of the spatial average pyroelectric voltage $\langle V_p^I(\omega) \rangle$ in Inverse detection is provided by the following equation:

$$\langle V_p^I(\omega) \rangle = \frac{2}{(jw\tau_e+1)(jw\tau_{th}+1)\sigma_p l_p} \times \frac{1}{(b_{gs}+1)(b_{pg}+1)} \times Z_s(w) \qquad (2)$$

In Eq.2, $Z_s(w)$ represents the complex electrical impedance of the sample, expressed as follows:

$$Z_s(w) = |Z_s(w)| \, exp\left(-j\varphi_{Z_s}(\omega)\right) = Z' - jZ''$$

where $|Z_s(w)|$ denotes the amplitude of the sample's electrical impedance, while $\varphi_{Z_s}(\omega)$ represents the phase of the sample's electrical impedance. Z' and Z'' correspond, respectively, to the real and imaginary parts of Z_s as a function of frequency f. From the experimental curves of the IEPE signal, which provide amplitude and phase information of AC impedance across frequencies f, ranging from 200 Hz to approximately 50 kHz, the complex impedance diagram ($Z'' = f(Z')$) of the sample is depicted. In the IEPE setup, the complex impedance of the sample is determined as a function of frequency, and subsequent AC to DC conductivity extrapolation is performed to yield the intrinsic electrical resistivity. The AC electrical conductivity σ_{AC} can be determined using the following equation: $\sigma_{AC} = \frac{L}{Z'A}$. Here, L represents the distance between electrodes (L = 1.5 cm), and A denotes the cross-sectional area (A = 1.5 cm²). Ultimately, the DC conductivity (resistivity respectively) is obtained through extrapolation at zero frequency from AC investigations.

III. EXPERIMENTAL SET-UP

Figure 2 presents the schematic diagram of the experimental setup used for EPE detection, as described in references [1]-[5]. In the EPE technique, the measurement process involves uniformly heating the samples using a sine-wave generator configured to produce electrical pulses, modulated at a specified frequency (f). The PVDF sensor is mounted on a 6 mm thick copper heat sink and connected to a current-to-voltage converter. The experimental setup is designed to be flexible, enabling the measurement of both the amplitude and phase of the photoacoustic (PE) signal across a modulation frequency range of 0.1 Hz to 50 kHz using a lock-in amplifier

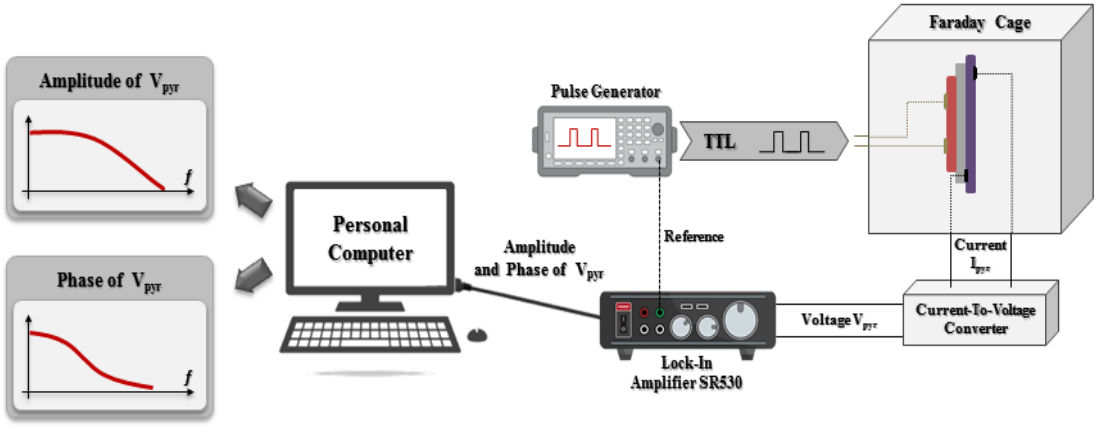

Fig. 2 The EPE Experimental set-up.

IV. RESULTS AND DISCUSSION:

The experimental validation focused on Cr:GaAs substrates, where Chromium doping enhances thermal stability, crucial for applications in 5G/6G systems [7]. The Cr:GaAs sample (360µm thick, [Cr]=10^{16} cm^{-3})

ISSN: 1737-9334

was grown by molecular-beam epitaxy (MBE)[8]. Figure 3. a show that the experimental curves remain stable at low frequencies, as the PVDF sensor operates as a resistive dipole until reaching 10 Hz, after which a slight decrease in signal amplitude occurs. This gradual reduction at higher frequencies indicates the anticipated dissipation of thermal waves due to phonon scattering, thereby confirming the sensitivity of the FEPE mode. The provided thermal parameters—κ_s = 52 ± 1.2 W/m·K and D_s = (0.33 ± 0.08) cm²/s—align closely (within 5% deviation) with first-principles predictions. The results are in good agreement with those documented in the literature at room temperature (~300K) [9]-[10].

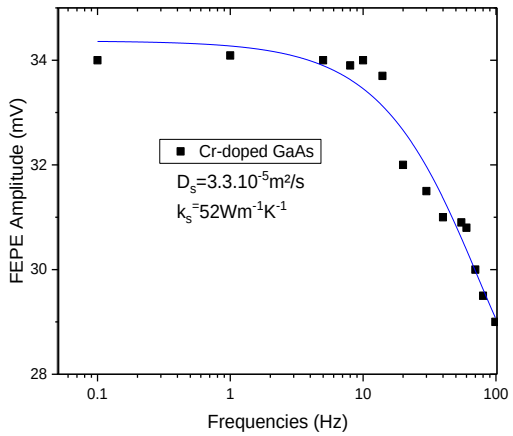

Fig. 3.a Thermal parameters of Cr:GaAs obtained from the FEPE configuration.

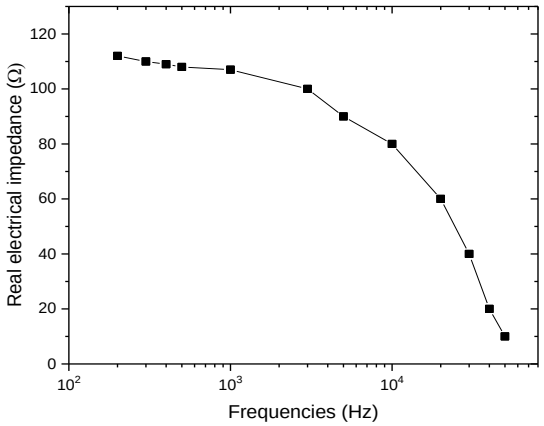

Fig 3.b Frequency dependence of the electrical impedance real-part (Z') from IEPE Detection.

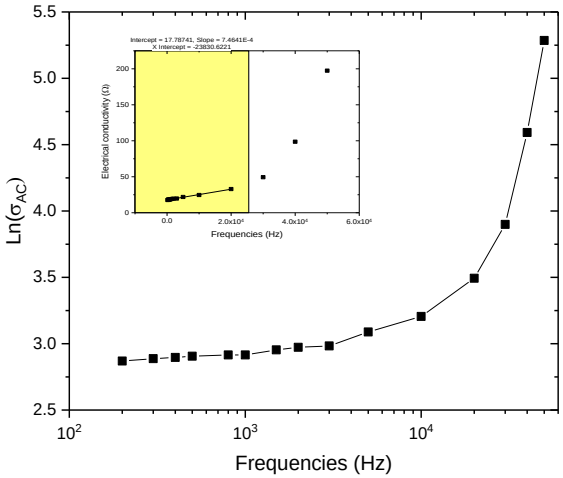

Fig. 3.c Electrical AC conductivity vs. frequency obtained from the IEPE configuration.

Having established the reliable measurement of the thermal parameters using the FEPE configuration, we now turn to the Inverse EPE (IEPE) setup to integrate these thermal measurements into an impedance framework for the precise determination of electrical resistivity. Fig. 3.b presents the real part (Z') of the response in the IEPE setup for the analyzed sample over a modulation frequency range of roughly 200 Hz to 50 kHz. The IEPE mode provided a detailed frequency-dependent behavior of the real component of the electrical impedance, Z'. The decrease in Z' with increasing frequency suggests notable capacitive effects that influence electrical conduction. To elaborate on these results, Fig. 3.c depicts the natural logarithm of the AC electrical conductivity ($Ln\sigma_{AC}$) changes across the operational frequency spectrum. The obtained electrical resistivity (σ = 17.78 ± 0.45 S/m, ρ = 0.056 ± 0.001 Ω·m) aligns with the anticipated behavior of ideal semi-insulating substrates. Compared to undoped GaAs, the increased electrical conductivity in Cr-doped GaAs suggests the

ISSN: 1737-9334

potential for exploring alternative doping strategies to enhance electron mobility. The literature value for undoped GaAs is approximately 1 S/m, and existing studies indicate that the conductivity has increased by more than 50% [11]. Although the moderate resistivity of Cr-doped GaAs restricts its use in active layers, its thermal-electrical properties make it highly suitable for thermal interface layers in 5G massive MIMO antennas, radiation-hardened substrates for satellite payloads, and THz modulators that rely on ultrafast carrier trapping via Cr^{3+} defects.

V. CONCLUSIONS

The EPE methodology can be tailored to integrate novel material systems suitable for next-generation electronics and advanced semiconductor substrates exceeding 10 μm in thickness with doping densities ranging from 10^{15} to 10^{18} cm^{-3}. Its rapid measurement acquisition, high precision, and cost-effectiveness enhance its scalability for industrial applications. Future research should focus on optimizing the thermal and electrical characteristics of 2D materials integrated with wide-bandgap semiconductors to support emerging technologies such as 6G and quantum computing [12]. These improvements are anticipated to stimulate further debate and innovation in the field, providing a robust platform for developing more advanced semiconductor devices.

REFERENCES

[1] I. Mellouki et al., Thermochimica Acta, vol. 670, pp. 123–127, 2018.
[2] A. Mami et al., Int. J. Eng. Sci. Innov. Technol., vol. 3, no. 3, pp. 608–617, 2014.
[3] D. Wang et al., Applied Physics Reviews, vol. 11, article 021407, 2024.
[4] O. Andrzej, Processing of signal of pyroelectric sensor in laser energy meter, Measurement Science Rev., vol. 1, no. 1, pp. 215–218, 2001.
[5] A. Mami, R. Boughalmi, S. Lazzez, I. Mellouki, N. Yacoubi, and M. Amlouk, Determination of thermal properties of some sulfide thin films using the electropyroelectric method, Journal of Thermal Analysis and Calorimetry, vol. 136, pp. 2231–2238, 2019.
[6] N. Bennaji, I. Mellouki, and N. Yacoubi, Thermal properties of metals using the photopyroelectric technique: Electrical heating, Sensor Letters, vol. 7, pp. 716–720, 2009.
[7] T. W. Hickmott, IEEE Transactions on Electron Devices, vol. 31, no. 1, pp. 54–62, 1984.
[8] C. T. Foxon, Molecular Beam Epitaxy. In: C. R. Leavens and R. Taylor, Eds., Interfaces, Quantum Wells, and Superlattices, NATO ASI Series, vol. 179, Springer, Boston, MA, 1988.
[9] Jong Tae Lim, Joong Gill Choi, Yong Hwan Bak, Seung Han Park, and Ung Kim, Photoacoustic investigation of the carrier transport processes and the thermal properties in n-type GaAs, Journal of the Korean Physical Society, vol. 31, no. 4, pp. 608–612, 1997.
[10] A. Ghukasyan, P. Oliveira, N. I. Goktas, and R. LaPierre, Thermal conductivity of GaAs nanowire arrays measured by the 3ω method, Nanomaterials, vol. 12, article 1288, 2022, doi:10.3390/nano12081288.
[11] C. de Freitas Bueno et al., Photo-induced conductivity of heterojunction GaAs/rare-earth doped SnO_2, Materials Research, vol. 16, no. 4, pp. 831–838, 2013.
[12] G. Krishnamoorthy, X. Hu, J. Park, and D. Lee, Opportunities and challenges of integrating 2D materials with wide-bandgap semiconductors for next-generation electronics, ACS Applied Materials & Interfaces, vol. 15, no. 5, pp. 6103–6114, 2023.

ISSN: 1737-9334